Supporting Information

Enhanced Photocatalytic CO_2 Reduction with Photothermal Effect by Cooperative Effect of Oxygen Vacancy and Au Cocatalyst

Songcai Cai,[†,§] Jing Chen,[‡,§] Qiang Li,[†,§] and Hongpeng Jia*[,†,§]

[†] CAS Center for Excellence in Regional Atmospheric Environment, and Key Laboratory of Urban Pollutant Conversion, Institute of Urban Environment, Chinese Academy of Sciences, Xiamen 361021, China

[‡] CAS Key Laboratory of Design and Assembly of Functional Nanostructures, and Fujian Provincial Key Laboratory of Nanomaterials, Fujian Institute of Research on the Structure of Matter, Chinese Academy of Sciences, Fuzhou 350002, China

[§] University of Chinese Academy of Sciences, Beijing 100049, China

1. Experimental section

1.1 Characterization. Inductively coupled plasma optical emission spectrometer (ICP-OES) was used to analyze the actual Au content in different samples. Nitrogen adsorption-desorption isotherms were measured on the Quantachrome instrument (Autosorb IQ), in which the Brunauer-Emmett-Teller (BET) and Barrett-Joyner-Halenda (BJH) methods were employed to determine the specific surface area (S_{BET}) and pore size distribution (D_{BJH}), respectively. X-ray diffraction (XRD) patterns were collected on an X'Pert Pro diffractometer with a Cu-Kα radioactive source (40 kV, 40 mA). Raman spectra were recorded on a micro-Raman spectrometer (LabRAM Aramis) with a λ = 532 nm laser as the excitation source. X-ray photoelectron spectroscopy (XPS) measurements were performed on a Kratos/Shimadzu AXIS Supra instrument. Field emission scanning electron microscopy (SEM) images were obtained from the Hitachi S-4800 instrument. Transmission electron microscopy (TEM) images, high-resolution transmission electron microscopy (HRTEM) images, high angle annular dark-field scanning transmission electron microscopy (HAADF-STEM) images, and energy-dispersive X-ray spectroscopy (EDS) were obtained using JOEL 2100F instrument. The UV-vis diffuse reflectance spectra (UV-vis DRS) were acquired with a Shimadzu UV-2500 spectrophotometer. Electron paramagnetic resonance (EPR) spectroscopy was carried out on an A300 spectrometer at liquid nitrogen, where 10 mg of powder was weighed and put into the sample tube for testing. Photoluminescence (PL) spectrum was recorded by a fluorescence spectrophotometer (Hitachi F-4600) with 300 nm excitation light. The photoelectrochemical (PEC) analysis was conducted

on an electrochemical workstation (CHI660D, CH Instruments Inc., China). The detailed operation procedure can refer to our previous work.[1]

1.2 Photothermocatalytic CO_2RR. The photothermocatalytic reduction of CO_2 with H_2O vapor was achieved in a closed stainless-steel reactor with a volume of 227 mL under full-spectrum irradiation (PLS-SXE300UV, PerfectLight) or infrared light (IR lamp, PHILIPS IR 375W). The UV cut-off filter was used to get the vis-IR light. The light intensity was detected by an optical power meter (CEL-NP2000-2, PerfectLight). For all experiments, 10 mg of catalyst was coated on a fiberglass membrane and put inside of the reactor. A thermocouple was put on the catalyst layer to detect the surface temperature. The humid CO_2 gas (5 vol.% H_2O) was introduced into the reactor for 1 h to ensure an anaerobic environment. Then the reactor was sealed to start light reaction for 2 h. The products of CO and CH_4 were periodically monitored on a gas chromatograph equipped with TCD and FID. Moreover, the yield rate and selectivity of products were calculated by the following equations.

$$\text{Yield rate of } C_i \text{ (mole/g)} = (\text{mole of } C_i)/(\text{wt. of catalyst})$$

$$\text{Selectivity of product } C_i \text{ (\%)} = (\text{mole of } C_i)/(\text{total moles of all products})$$

where C_i represents the carbon species (CO and CH_4).

In the low-temperature experiment, other operation steps are consistent with the above-mentioned except the reaction temperature regulated by an ice-water bath.

1.3 The concrete calculation process of the theoretical value of noble metal Au

$$x\ (\text{wt\%}) = 100M_1/(M_1+M_2)$$

x, M_1 and M_2 represent the mass percentage of loaded noble metal Au, the mass of

loaded noble metal Au, and the mass of loaded support, respectively.

2. Figures and Tables

Table S1. Physical properties and element composition of the samples.

Samples	S_{BET} (m^2/g)	D_{BJH} (nm)	Au content (wt%)
mTiO_2	87.57	11.41	-
*m*T-H2	83.62	11.42	-
*m*T-H4	87.14	11.35	-
*m*T-H6	42.33	15.54	-
0.1Au/*m*T-H6	43.75	13.14	0.097
0.25Au/*m*T-H6	48.32	11.43	0.245
0.5Au/*m*T-H6	49.14	11.38	0.528
0.75Au/*m*T-H6	45.31	13.16	0.669
1Au/*m*T-H6	32.47	23.99	1.054
0.5Au/*m*TiO_2	63.67	15.50	0.506

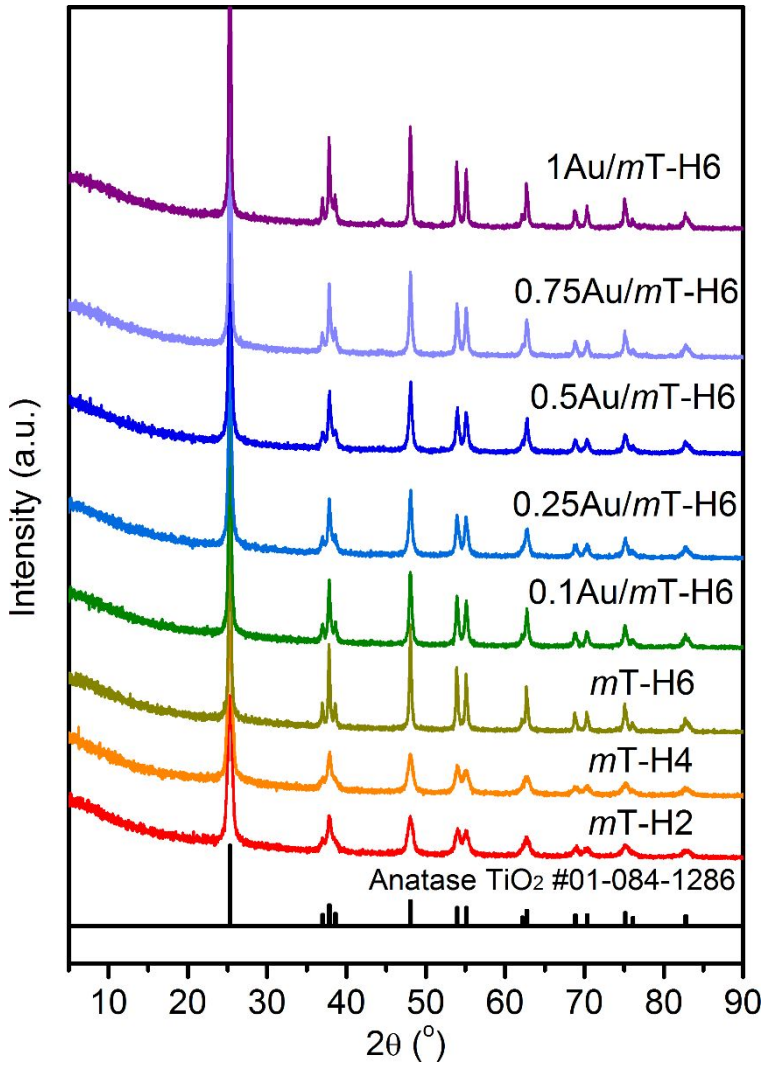

Figure S1. XRD patterns of the as-prepared samples.

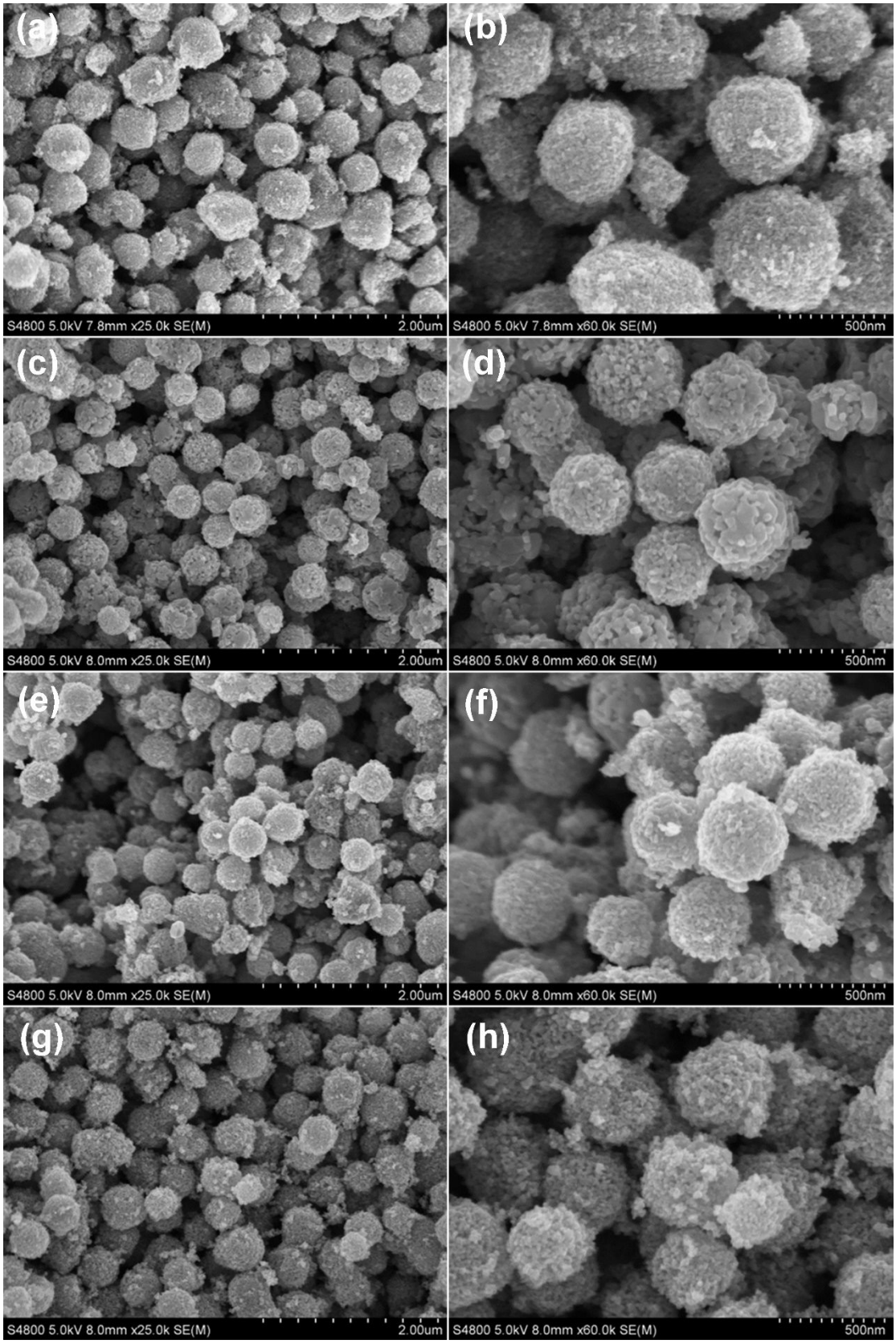

Figure S2. SEM images of the pristine *m*TiO_2 (a,b), *m*T-H6 (c,d), 0.5Au/*m*T-H6 (e,f) and 0.5Au/*m*TiO_2 (g,h).

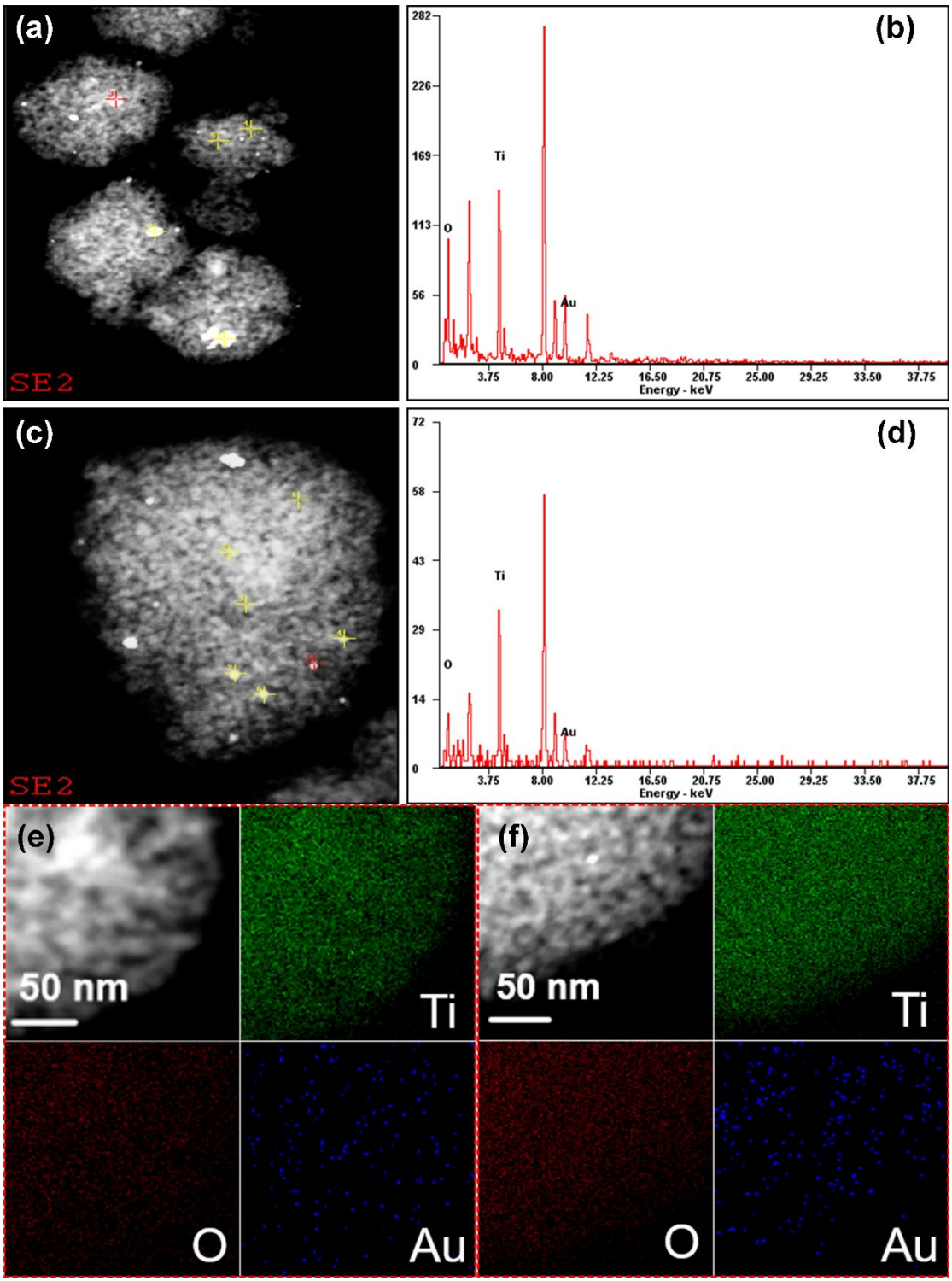

Figure S3. HAADF-STEM images and dot scanning of 0.5Au/*m*T-H6 (a,b) and 0.5Au/*m*TiO_2 (c,d). HAADF-STEM images and corresponding elemental mapping results of 0.5Au/*m*T-H6 (e) and 0.5Au/*m*TiO_2 (f).

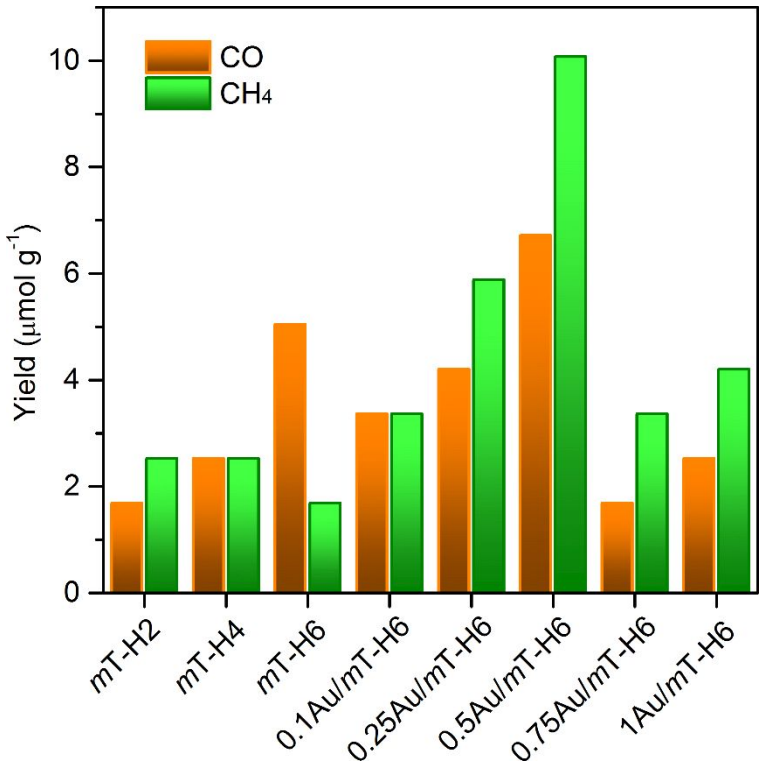

Figure S4. Yield of products and CO selectivity over the catalysts under irradiation of full spectrum light (0.72 W cm^{-2}) for 2 h (Reaction condition: humid CO_2 with 5 vol.% H_2O in a 227 mL closed reactor).

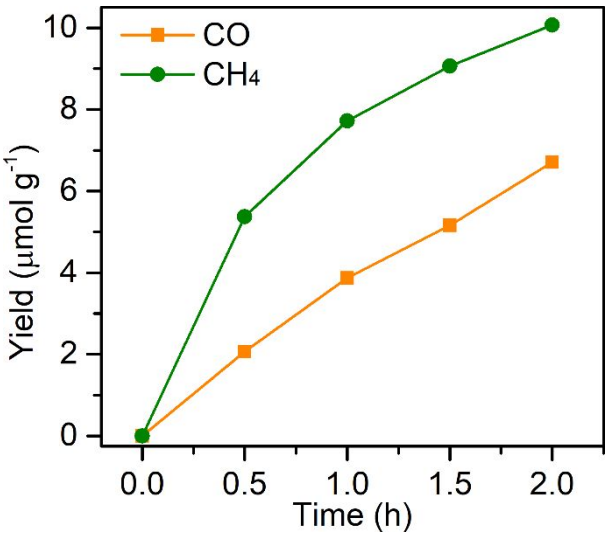

Figure S5. CO and CH_4 yields as a function of light irradiation time using 0.5Au/*m*T-H6.

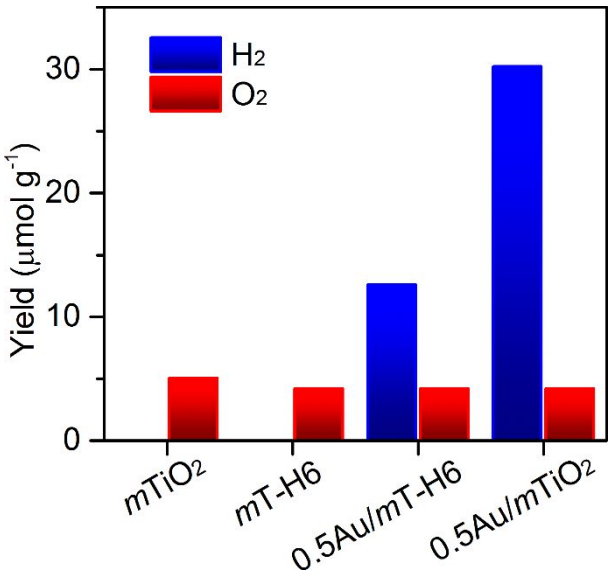

Figure S6. Yield of H_2 and O_2 over the catalysts under irradiation of full spectrum light (0.72 W cm^{-2}) for 2 h (Reaction condition: humid CO_2 with 5 vol.% H_2O in a 227 mL closed reactor).

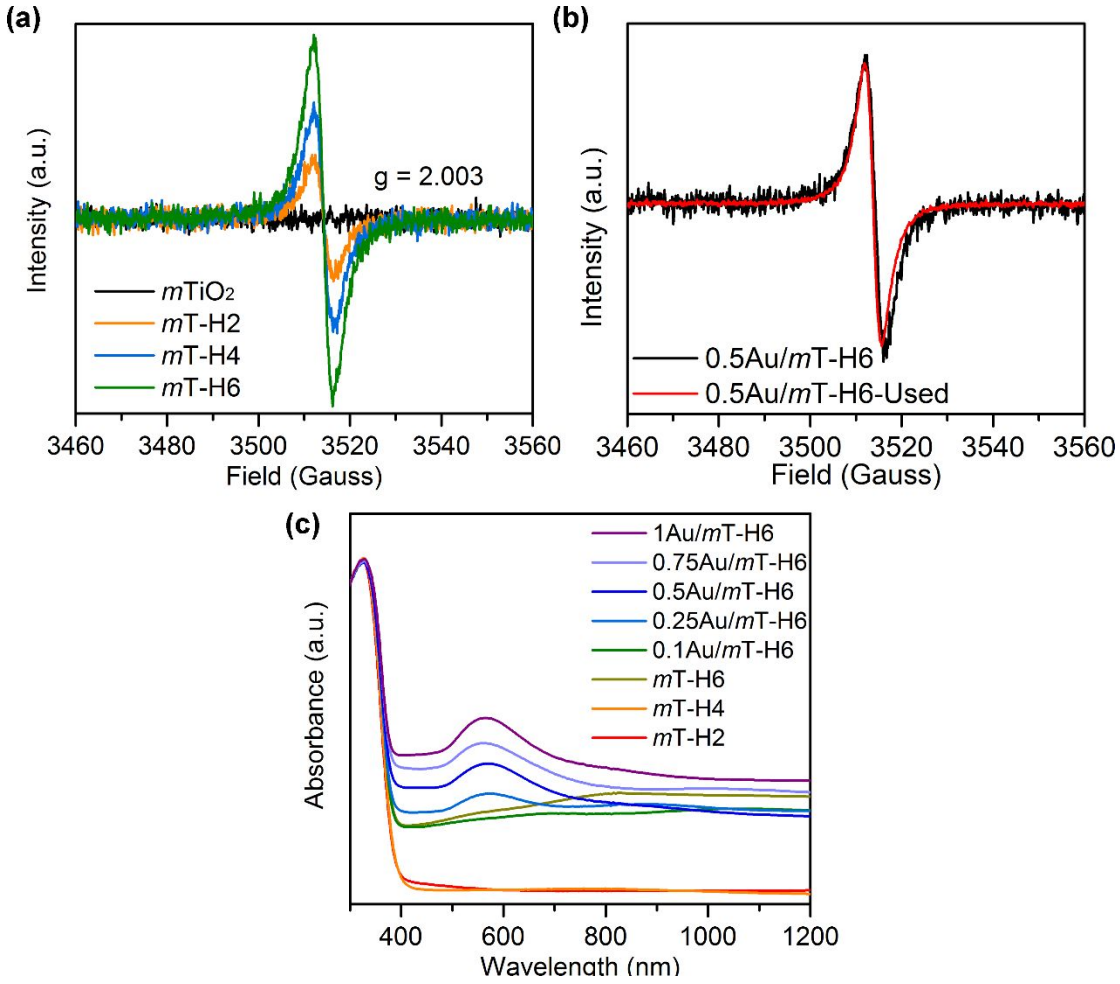

Figure S7. EPR spectra (a) of pristine *m*TiO_2 and hydrogenated *m*T-H6, EPR spectra before and after

stability test of the catalyst 0.5Au/*m*T-H6 (b), and DRS spectra (c) of the as-prepared samples.

Figure S8. The photographs of the as-prepared samples: pristine *m*TiO_2 (a), *m*T-H2 (b), *m*T-H4 (c), *m*T-H6 (d), 0.1Au/*m*T-H6 (e), 0.25Au/*m*T-H6 (f), 0.5Au/*m*T-H6 (g), 0.75Au/*m*T-H6 (h), 1Au/*m*T-H6 (i) and 0.5Au/*m*TiO_2 (j).

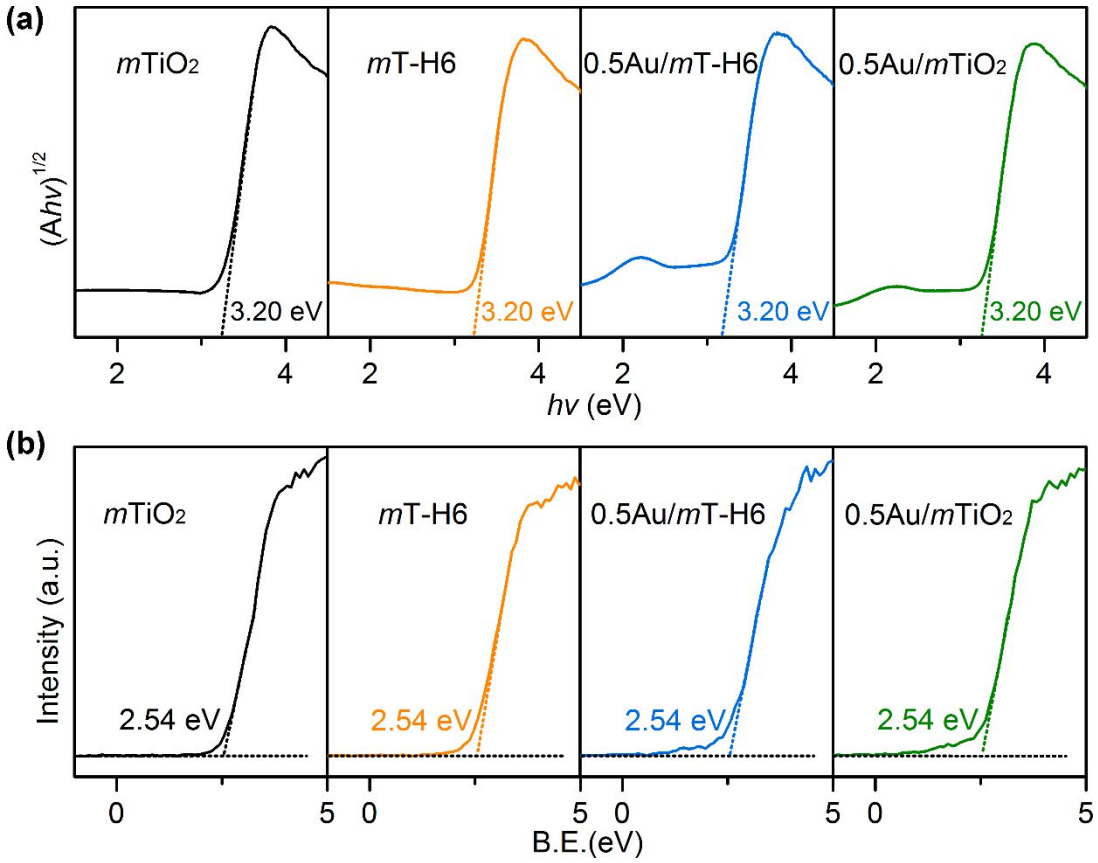

Figure S9. (A*hv*) *vs hv* curves (a) and XPS valence spectra (b) of *m*TiO_2, *m*T-H6, 0.5Au/*m*T-H6 and 0.5Au/*m*TiO_2.

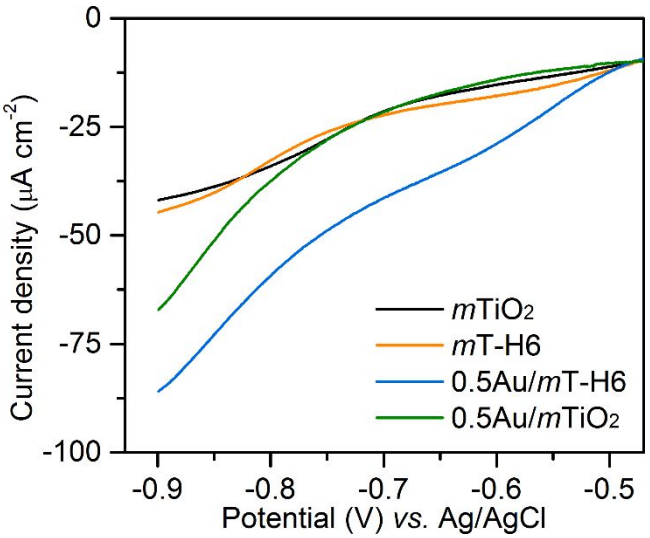

Figure S10. LSV curves of the as-prepared samples under irradiation.

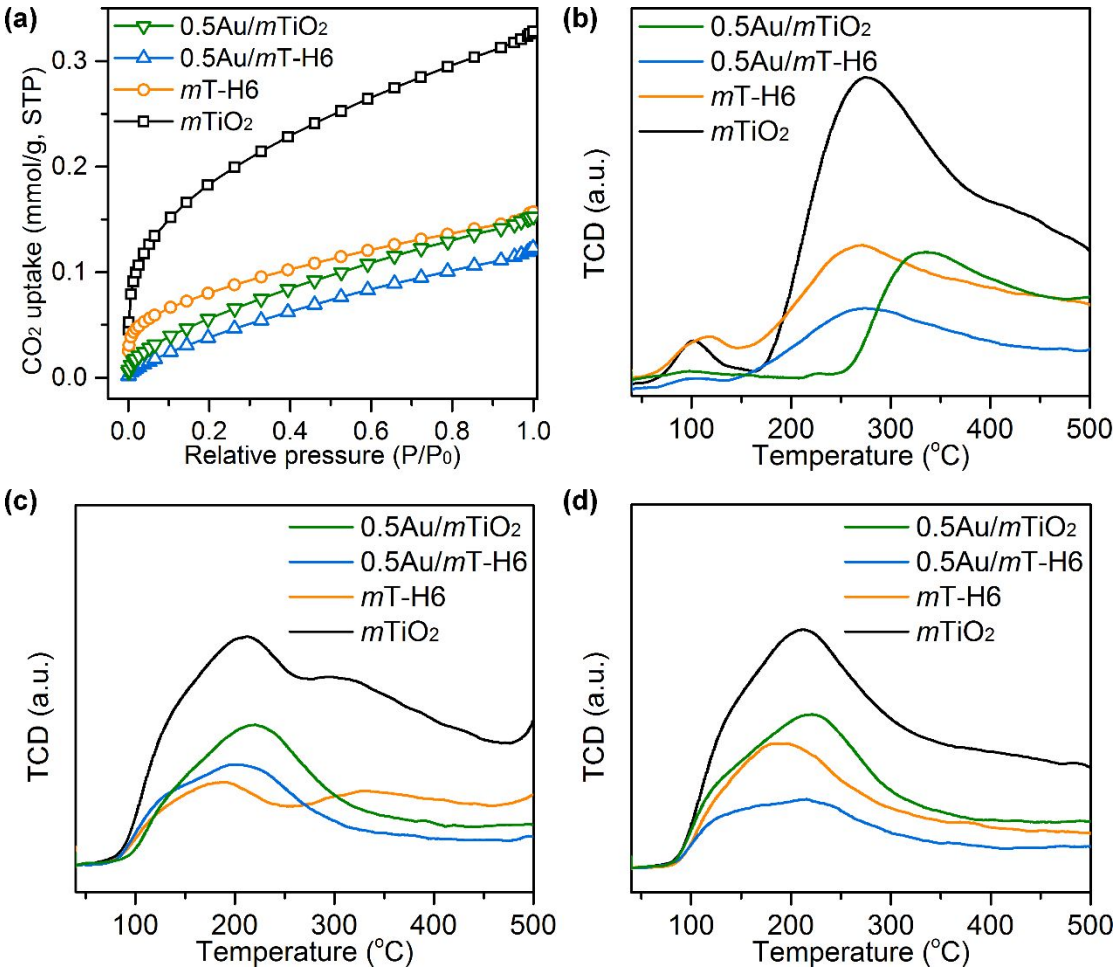

Figure S11. CO_2 uptake curves (a), CO_2-TPD (b), CO-TPD (c) and CH_4-TPD (d) of the samples.

References

(1) Cai, S.; Zhang, M.; Li, J.; Chen, J.; Jia, H. Anchoring Single-Atom Ru on CdS with Enhanced CO_2

Capture and Charge Accumulation for High Selectivity of Photothermocatalytic CO_2 Reduction to Solar Fuels. *Sol. RRL* **2020**, 2000313.